TISSUE ENGINEERING: Part C
Volume 16, Number 3, 2010

DOI: 10.1089/ten.tec.2009.0362

Cardiomyoblast-like Cells Differentiated from Human Adipose Tissue-Derived Mesenchymal Stem Cells Improve Left Ventricular Dysfunction and Survival in a Rat Myocardial Infarction Model

Hanayuki Okura, M.S.,[1–4] Akifumi Matsuyama, M.D., Ph.D.,[1] Chun-Man Lee, M.D., Ph.D.,[1,2] Ayami Saga, M.S.,[1] Aya Kakuta-Yamamoto, B.S.,[1] Anna Nagao, B.S.,[1,2] Nagako Sougawa, D.M.D., Ph.D.,[1] Naosumi Sekiya, M.D.,[3] Kazuhiro Takekita, M.S.,[1,2] Yashuhiro Shudo, M.D.,[3] Shigeru Miyagawa, M.D., Ph.D.,[3] Hiroshi Komoda, M.D., Ph.D.,[1,5] Teruo Okano, Ph.D.,[6] and Yoshiki Sawa, M.D., Ph.D.[2,3]

Adipose tissue–derived mesenchymal stem cells (ADMSCs) are multipotent cells. Here we examined whether human ADMSCs (hADMSCs) could differentiate into cardiomyoblast-like cells (CLCs) by induction with dimethylsulfoxide and whether the cells would be utilized to treat cardiac dysfunction. Dimethylsulfoxide induced the expression of various cardiac markers in hADMSCs, such as α-cardiac actin, cardiac myosin light chain, and myosin heavy chain; none of which were detected in noncommitted hADMSCs. The induced cells were thus designated as hADMSC-derived CLCs (hCLCs). To confirm their beneficial effect on cardiac function, hCLC patches were transplanted onto the Nude rat myocardial infarction model, and compared with noncommitted hADMSC patch transplants and sham operations. Echocardiography demonstrated significant short-term improvement of cardiac function in both the patch-transplanted groups. However, long-term follow-up showed rescue and maintenance of cardiac function in the hCLC patch-transplanted group only, but not in the noncommitted hADMSC patch-transplanted animals. The hCLCs, but not the hADMSCs, engrafted into the scarred myocardium and differentiated into human cardiac troponin I-positive cells, and thus regarded as cardiomyocytes. Transplantation of the hCLC patches also resulted in recovery of cardiac function and improvement of long-term survival rate. Thus, transplantation of hCLC patches is a potentially effective therapeutic strategy for future cardiac tissue regeneration.

Introduction

END-STAGE HEART FAILURE remains a major cause of death worldwide, with most cases due to ischemia. This is despite the remarkable progress in recent years in both medical and surgical treatments for heart failure. Cardiac transplantation and mechanical support using implantation of the left ventricular assist system were established as the ultimate means of support for these patients.[1,2] However, these treatment entities have limitations including donor shortage, rejection, and left ventricular assist system durability, and alternative strategies are needed in such circumstances.

Cellular cardiomyoplasty was developed as a new approach to restore impaired heart function,[3,4] using a variety of cell types, with encouraging initial results.[3–5] Mesenchymal stem cells (MSCs) seem particularly advantageous for cellular therapy in general because they are multipotent, potentially immune privileged,[6] and expand easily *ex vivo*. MSCs also proliferate rapidly, induce angiogenesis, and can differentiate into cardiomyogenic cells.[7–10] An MSC population was recently isolated from human adipose tissue, which is abundantly available and can be resected easily and safely in most patients.[11,12] These adipose tissue-derived cell lineages showed cardiomyocytic differentiation and rescued

[1]Department of Somatic Stem Cell Therapy, Foundation for Biomedical Research and Innovation, Kobe, Japan.
[2]Medical Center for Translational Research, Osaka University Hospital, Suita, Japan.
[3]Department of Surgery, Osaka University Graduate School of Medicine, Suita, Japan.
[4]Research Fellow of the Japan Society for the Promotion of Science, Tokyo, Japan.
[5]Department of Internal Medicine, National Hospital Organization Chiba Medical Center, Chiba, Japan.
[6]Institute of Advanced Biomedical Engineering and Science, Tokyo Women's Medical University, Tokyo, Japan.

cardiac dysfunction in a myocardial infarction (MI) animal model. Thus, the adipose tissue is a convenient and preferred source of stem cell recovery for cardiac therapy. Recently, transplantation of monolayered adipose tissue-derived MSCs (ADMSCs) into MI rats reversed wall thinning in the scarred area and improved cardiac function in a short term, with the engrafted sheet of cells forming a thick stratum containing newly formed vessels and scattered cardiomyocytes derived from the implanted cells.[13] As patients with severe heart failure desire sustained and long-term recovery of cardiac function after treatment rather than short-term improvement, continued efforts should be made to develop cell transplants from ADMSCs that survive and differentiate into cardiomyocytes *in vivo* for subsequent engraftment onto scarred myocardium.

This study investigated the differentiation of human ADMSCs (hADMSCs) into cardiomyoblast-like cells (CLCs) *in vitro*, analyzed the functional and histological regeneration of damaged myocardium after transplantation of CLCs *in vivo*, and examined the effects of such transplantation on long-term patient survival.

Materials and Methods

Adipose tissues from human subjects

Excess omental adipose tissues were resected from the gastro-omental artery during coronary artery bypass graft surgery and gastrectomy in 10 subjects [4 men and 6 women; age, 55 ± 5 years, mean ± standard error of mean (SEM); range, 40–60 years]. All subjects provided informed consent, and the Review Board for Human Research of Osaka University Graduate School of Medicine approved all protocols. All subjects fasted for at least 10 h before surgery and none was on steroid therapy at the time of surgery. Ten to 50 grams of adipose tissue was obtained from each subject.

Isolation of hADMSCs and differentiation into CLCs

hADMSCs were obtained as reported previously, with modification.[11,14] Briefly, the resected excess adipose tissue was minced and then digested at 37°C for 1 h in Hank's balanced salt solution (Gibco–Invitrogen, Grand Island, NY) containing 0.075% collagenase type II (Sigma–Aldrich, St. Louis, MO). Digests were filtered through a cell strainer (BD Bioscience, San Jose, CA) and centrifuged at 800 *g* for 10 min. Red blood cells were excluded using density gradient centrifugation with Lymphoprep ($d = 1.077$; Nycomed, Oslo, Norway), and the remaining cells were cultured in Dulbecco's modified Eagle's medium (Gibco–Invitrogen) with 10% defined fetal bovine serum (Hyclone, Logan, UT) for 24 h at 37°C. Following incubation, the adherent cells were washed extensively and then treated with 0.2 g/L ethylenediaminetetraacetate solution (Nacalai Tesque, Kyoto, Japan). The resulting suspended cells were replated at a density of 10,000 cells/cm^2 on human fibronectin-coated dishes (BD BioCoat, Franklin Lakes, NJ) in 60% Dulbecco's modified Eagle's medium-low glucose, 40% MCDB-201 medium (Sigma–Aldrich), 1×insulin-transferring selenium (Gibco–Invitrogen), 1 nM dexamethasone (Sigma–Aldrich), 100 μM ascorbic acid 2-phosphate (Sigma–Aldrich), 10 ng/mL epidermal growth factor (PeproTec, Rocky Hill, NJ), and 5% fetal bovine serum. After passaging five to six times in the same medium, the hADMSCs were used for transplantation. Cardiomyocytic differentiation was achieved by inducing hADMSCs with 0.1% dimethylsulfoxide (DMSO) for 48 h, resulting in a population named CLCs.

Reverse transcriptase–polymerase chain reaction

Total RNA was isolated from hADMSCs and cardiomyoblasts using an RNAeasy kit (Qiagen, Hilden, Germany). As a control, excess human myocardium was resected during maze surgery from 10 matched subjects (4 men and 6 women; age, 55 ± 5 years, mean ± SEM; range, 40–60 years) with informed consent. Control subjects also fasted for at least 10 h before surgery, and none was taking steroids. Approximately 1 g of myocardium was obtained from each subject, and the same protocol was performed to obtain total RNA. After treatment with DNase, cDNA was synthesized from 500 ng total RNA using Superscript III reverse transcriptase RNase H minus (Invitrogen, Carlsbad, CA). The absence of DNA contamination in RNA samples was confirmed with polymerase chain reaction (PCR) primers flanking an intron. Primers and the reaction conditions are described in Table 1. The PCR products were fractionated by 2% agarose gel electrophoresis.

Table 1. Primers Used in Reverse Transcriptase–Polymerase Chain Reaction

Primer		*Sequence*	*No. of cycles*	*Annealing temperature (°C)*
GAPDH	Forward	GTCAGTGGTGGACCTGACCT	35	60
	Reverse	AGGGGAGATTCAGTGTGGTG		
Islet-1	Forward	TGATGAAGCAACTCCAGCAG	35	60
	Reverse	GGACTGGCTACCATGCTGTT		
Nkx2.5	Forward	GGTGGAGCTGGAGAAGACAGA	35	60
	Reverse	CGACGCCGAAGTTCACGAAGT		
GATA-4	Forward	ACCAGCAGCAGCGAGGAGAT	35	60
	Reverse	GAGAGATGCAGTGTGCTCGT		
α-Cardiac actin	Forward	GGAGTTATGGTGGGTATGGGTC	35	60
	Reverse	AGTGGTGACAAAGGAGTAGCCA		
Myosin light chain-2v	Forward	5′-GCGCCAACTCCAACGTGTTCT	35	60
	Reverse	5′-GTGATGATGTGCACCAGGTTC		
Myosin heavy chain	Forward	GGGGACAGTGGTAAAAGCAA	35	60
	Reverse	TCCCTGCGTTCCACTATCTT		

Model animals for MI

The left anterior descending coronary artery of rats with severe combined immunodeficiency was ligated. In brief, rats were anesthetized with nembutal (40 mg/kg), before being intubated and ventilated at a rate of 60 cycles/min with a tidal volume of 5 mL under room air supplemented with oxygen (2 L/min). The hearts were exposed through the fifth left-intercostal space and the left anterior descending was ligated. After 4 weeks, the hearts were again exposed through the fifth left-intercostal space, and the infarct area was identified visually based on surface scarring and abnormal wall motion. Cell sheets were subsequently implanted onto the infarcted myocardium. The control group was treated similarly, but no cell sheets were implanted. The Osaka University Graduate School of Medicine Standing Committee on Animals approved all experimental protocols.

Preparation of monolayered cell sheets

After four to five passages, the hADMSCs were trypsinized and then replated onto 35-mm temperature-responsive dishes (CellSeed, Tokyo, Japan) in 2 mL of expansion medium at 1×10^6 cells per dish. After culture at 37°C for 2 days, 0.1% DMSO was added to the medium on half of the dishes to differentiate the hADMSCs into cardiomyoblasts. After 2 days of culture, the cells were incubated again at 20°C. Within 20 min, the hADMSCs and CLC sheets detached spontaneously and floated up into the medium for use as monolayered cell grafts.[13,15–17]

Assessment of rat cardiac function

Cardiac ultrasound studies were performed before ligation, before implantation, and at 2, 4, 8, 10, 12, 14, and 16 weeks after implantation using a SONOS 7500 (Philips Medical Systems, Andover, MA). Plasma atrial natriuretic protein (ANP) level was analyzed using an ANP ELISA system (Phoenix Pharmaceuticals, Burlingame, CA) by following the instructions supplied by the manufacturer.

Histological analyses

The rat hearts were dissected out and immediately fixed overnight in 4% paraformaldehyde, washed in 70% alcohol, dehydrated through a graded ethanol series, cleared in xylene, and finally processed for embedding in paraffin wax. Paraffin sections were cut at 5 μm thickness, delineated on the microscope slide using a Dako pen (Dako, Glostrup, Denmark), deparaffinized in xylene, and then rehydrated through a graded ethanol series into distilled water. The sections were then immersed in Target Retrieval Solution (Dako) in distilled water and boiled, followed by cooling at room temperature for 20 min. The sections were then washed in two changes of Tris-buffered saline (TBS), pH 7.4, followed by 1% polyoxyethylene sorbitan monolaurate (Tween 20) in TBS (TBS-T), and then an overnight incubation with 10% Blocking One® (Nacalai Tesque) in TBS-T. The sections were then incubated in a humid chamber for 16 h at 4°C with mouse monoclonal antibodies to α-cardiac actin (α-CA) and human troponin I, diluted in the blocking solution, followed by Alexa Fluor 546-labeled donkey anti-goat IgG (Molecular Probes, Eugene, OR). The stained slides were viewed on a BioZero laser scanning microscope (Keyence, Osaka, Japan).

Statistical analysis

All data were expressed as mean ± SEM. Differences between groups were analyzed for statistical significance by the Student's *t*-test using SPSS Statistics 17.0 (SPSS, Inc., Chicago, IL). A *p*-value less than 0.05 denoted a statistically significant difference. Survival curves were constructed by the Kaplan–Meier method and survival among groups was compared using the Log-Rank test (StatMate III for Windows; Atoms, Tokyo, Japan).

Results

Cardiac differentiation of hADMSCs into CLCs

The potential for hADMSCs to differentiate into CLCs was evaluated from the mRNA expression of several cardiac differentiation markers by reverse transcriptase-PCR before and after DMSO induction, as follows: *islet-1* is a cardiac stem cell marker; *Nkx2.5* and *GATA-4* are transcription factors required for subsequent cardiac differentiation; and *α-CA*, *myosin light chain*, and *myosin heavy chain* (*MHC*) are markers of cardiac differentiation (Fig. 1A). Preinduced hADMSCs expressed *islet-1* and *Nkx2.5* mRNA, but not that of *GATA-4*, *α-CA*, *myosin light chain*, or *MHC*. After induction by DMSO for 48 h, hADMSCs expressed all markers, indicating that DMSO treatment successfully differentiated hADMSCs into cells of the cardiac lineage, and these induced cells were named CLCs.

Preparation and transplantation of hADMSC-derived CLC patches

To evaluate the potential therapeutic usefulness of CLCs, we designed an experimental rat model of coronary ligated infarction to assess cardiac function after transplantation of CLC patches. CLC and control hADMSC patches were prepared from cell sheets, as described earlier (Fig. 1B). These patches were transplanted onto the scarred area of the left ventricular wall in the MI model Nude rats, whose left anterior descending artery had been ligated 4 weeks before graft implantation (Fig. 1C, D). Sham transplantations were also performed.

Effects of CLC transplantation on cardiac function and survival rate

Cardiac function was assessed by echocardiography at preligation, pretransplantation, and every 2 weeks after transplantation (Fig. 1D). Sixteen weeks after transplantation, the treated animals were sacrificed and cardiac tissues prepared for histological examination. Four weeks after graft implantation, wall motion was improved in both control and CLC patch-implanted hearts. However, the wall motion of control and noncommitted hADMSC patch-transplanted heart tissue was exacerbated at 16 weeks after transplantation, while improved motion was maintained with the CLC patch transplants (Fig. 2A). In the early phases of the post-transplantation period, left ventricular diastolic dimension was significantly reduced in both the transplanted groups, but by 8 weeks after implantation this parameter increased in the control hADMSC patch-transplanted group, whereas it remained unchanged in those animals that received CLC patch transplants (Fig. 2B). Likewise, left ventricular ejection

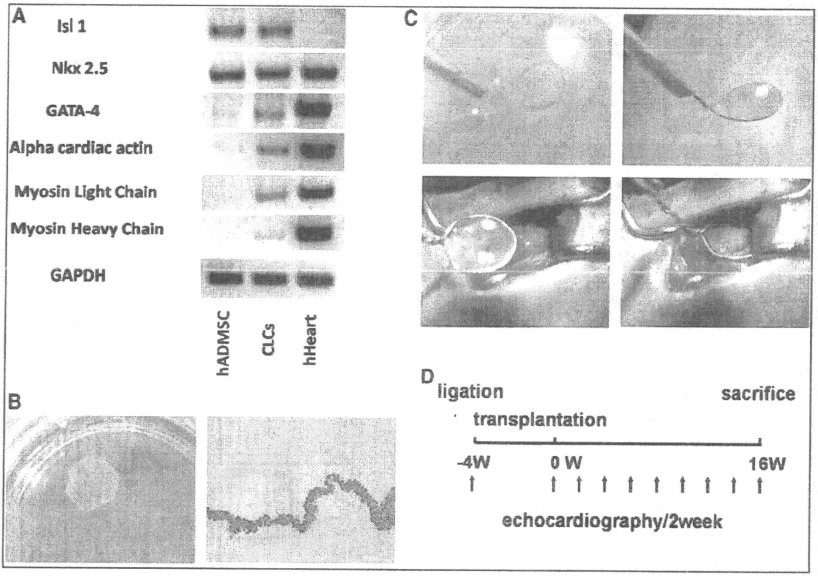

FIG. 1. Preparation and transplantation of human adipose tissue-derived mesenchymal stem cell (hADMSC)-derived cardiomyoblast-like cell (hCLC) patches. (**A**) Treatment with dimethylsulfoxide (DMSO) transformed hADMSCs into CLCs. The mRNA expressions of *islet-1*, *Nkx2.5*, *GATA-4*, *α-cardiac actin* (*α-CA*), *myosin light chain* (*MLC*), and *MHC* were analyzed by reverse transcriptase–polymerase chain reaction. The mRNAs for *islet-1* and *Nkx2.5*, with trace levels of *GATA-4* and *α-CA*, were expressed in hADMSCs, but no expression of *MLC* or *MHC* was detected. After induction with DMSO for 48 h, the hADMSCs also expressed *MLC* and *MHC*, indicating a phenotypic change into CLCs. (**B**) Preparation of hADMSC-derived CLC patches. The hADMSCs were cultured on temperature-responsive dishes for 48 h with 0.1% of DMSO for differentiation into CLCs. As the culture temperature was decreased from 37°C to 20°C, the CLCs detached spontaneously as sheets and floated up within 30 min into the culture media as a layered CLC patch. (**C**) Transplantation of hADMSC-derived CLC patches. Detached patches were transplanted onto the left ventricular wall scar in the myocardial infarction (MI) model Nude rats. (**D**) Protocol used for assessment of cardiac function. The left anterior descending artery was ligated in Nude rats at 4 weeks before graft implantation. Cardiac function was assessed by echocardiography at preligation, pretransplantation, and every 2 weeks following transplantation. The treated animals were sacrificed 16 weeks after transplantation and prepared for histological examination.

fractions improved in both the implanted groups until 8 weeks, after which time it worsened only in the group transplanted with noncommitted hADMSC patches (Fig. 2B).

ANP was then measured to confirm that chronic heart failure due to MI could be treated by CLC patch transplantation (Fig. 2C). The ANP levels were significantly increased after MI in all groups (Fig. 2C). The sham-operated MI control group showed incremental increases in plasma ANP over the time course of examination, whereas both CLC patch- and hADMSC patch-transplanted animals had low ANP levels until 8 weeks after treatment. However, ANP levels increased subsequently in the hADMSC patch-transplanted group, whereas the CLC patch-transplanted group maintained the improvement in ANP levels.

The Kaplan–Meier survival curve showed higher long-term survival rates in cell patch-transplanted groups than in sham-operated MI controls (Fig. 2D). Notably, no rat died after transplantation of an hADMSC-derived CLC patch. Survival at 16 weeks after surgery was 100% for the CLC group, 80% for the hADMSC group, and 16% for the sham-operated group, with a significant difference between the two transplanted groups. These results suggest that transplantation of hADMSC-derived CLCs has beneficial effect in rats with heart failure induced by MI.

Effects of CLC transplantation on cardiac structure

Cardiac structure was next examined histologically to analyze further the difference between CLC patch- and noncommitted hADMSC patch-transplanted animals in the longer term (Fig. 3). On hematoxylin and eosin and Masson trichrome staining, the sham-transplanted MI control rats

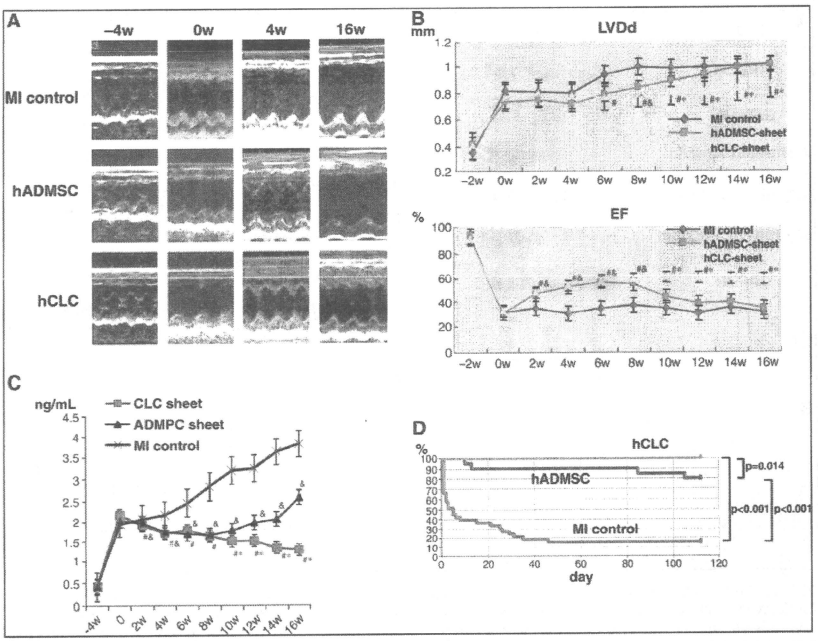

FIG. 2. Effects of CLC patch transplantation on cardiac function and long-term survival. (**A**) In both the patch-transplanted groups, echocardiography showed improved wall motion within 4 weeks of transplantation. However, at 16 weeks after transplantation, the wall motion of noncommitted hADMSC patch-transplanted rats worsened, whereas it was maintained in the CLC patch-transplanted animals. (**B**) Left ventricular diastolic dimension and ejection fractions improved significantly in both the patch-grafted groups in the early phase, as confirmed by echocardiography. However, these two parameters of cardiac function worsened at 8 weeks after implantation in the noncommitted hADMSC patch-transplanted groups, but not in the CLC patch-transplanted group. The numbers of all groups were five. Data are mean ± standard error of mean ($^{\#}p < 0.05$; MI control vs. the hCLC patch-transplanted animals; $^{\&}p < 0.05$; MI control vs. the noncommitted-hADMSC patch-transplanted rats; $^{*}p < 0.05$; hCLC patch-transplanted vs. the noncommitted hADMSC patch-transplanted rats, respectively). (**C**) Plasma ANP levels. Sham-operated MI control group showed increment of plasma ANP levels during the course of the experiment. Both the CLC patch- and hADMSC patch-transplanted groups showed suppression of ANP level increment till 8 weeks after treatment. ANP levels of the hADMSC patch-transplanted group increased from 8 weeks after transplantation, but no change in ANP levels was noted in the CLC patch-transplanted group. The numbers of all groups were four. (**D**) Long-term survival of rats with chronic heart failure that received the CLC patch ($n = 28$), noncommitted hADMSC patch ($n = 20$), or sham operation ($n = 37$). The Kaplan–Meier survival curve demonstrated that no rat died after transplantation of hADMSC-derived CLC patch. The survival rate at 16 weeks after surgery was 80% for the hADMSC group versus 16% for the sham-operated group. Log-rank test; *p*-values are indicated. LVDd, left ventricular diastolic dimension.

showed only a thin layer of cardiac muscle and fibrotic tissues in the scarred anterior left ventricular wall (Fig. 3A, B). Rats implanted with noncommitted hADMSCs showed small patches of cardiac muscles over that seen in the control MI rats (Fig. 3C, D). On the other hand, the rats transplanted with CLC patches showed significant reversal of the infracted myocardium and a full cardiac muscle layer overlaying the transplanted area (Fig. 3E, F, arrowheads).

CLCs differentiate into cardiac muscle in situ

The *in situ* differentiation capacity of the implanted cell sheets into cardiomyocytes after grafting onto the scarred myocardium was assessed by immunohistochemical staining for α-CA and human troponin I (Fig. 4). Thin layers of α-CA-positive cells were observed on the scarred myocardium of sham-operated MI control rats (Fig. 4A). A similar but thicker

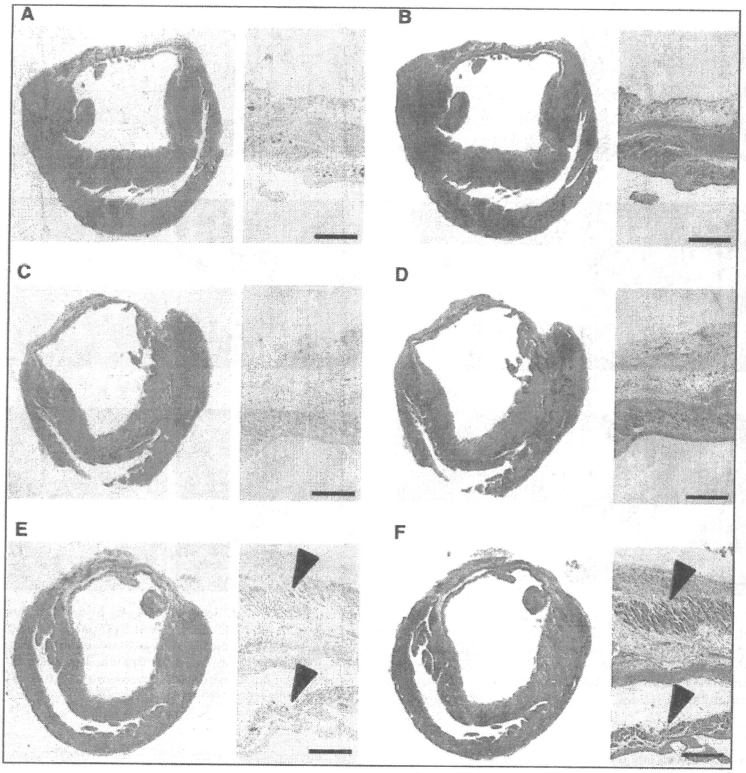

FIG. 3. Effects of CLC transplantation on cardiac structure. Photomicrographs showing representative myocardial sections stained with hematoxylin and eosin (**A, C, D**) and Masson trichrome (**B, D, F**) in the individual groups. The transplanted CLC patch reversed wall thinning of the infracted myocardium and another cardiac muscle was layered onto the transplanted area (arrowheads). (**A, B**) Sham-operated MI control group; (**C, D**) noncommitted hADMSC patch-transplanted group; and (**E, F**) hADMSC-derived CLC patch-transplanted group. Bars = 200 μm.

layer of α-CA-positive cells was apparent in the tissues from noncommitted hADMSC-transplanted rats (Fig. 4A, C), whereas the CLC patch-transplanted group showed two cardiac muscle layers positive for α-CA (Fig. 4E, arrow and arrowhead). There were no human troponin I-positive cells in the sham-operated MI control group (Fig. 4B), but some were observed in the noncommitted hADMSC patch-transplanted group (Fig. 4D). As shown in Figure 4F, large amounts of human troponin I-positive myocardium was observed in the CLC-transplanted animals (arrow) in addition to some human troponin I-negative but α-CA-positive myocardium in the internal myocardial layer (Fig. 4E, F, arrowhead). These results indicated that CLCs can efficiently differentiate into cardiomyocytes *in situ*.

Discussion

There are several advantages to hADMSC-derived CLC patch transplantation for regeneration therapy. First, the source of adipose-derived cells is easily and safely accessible and the cells can be obtained in large quantities, without serious ethical issues. Second, hADMSCs differentiate into CLCs by induction with DMSO, which is available in current good manufacturing practice grade. Third, hADMSC-derived

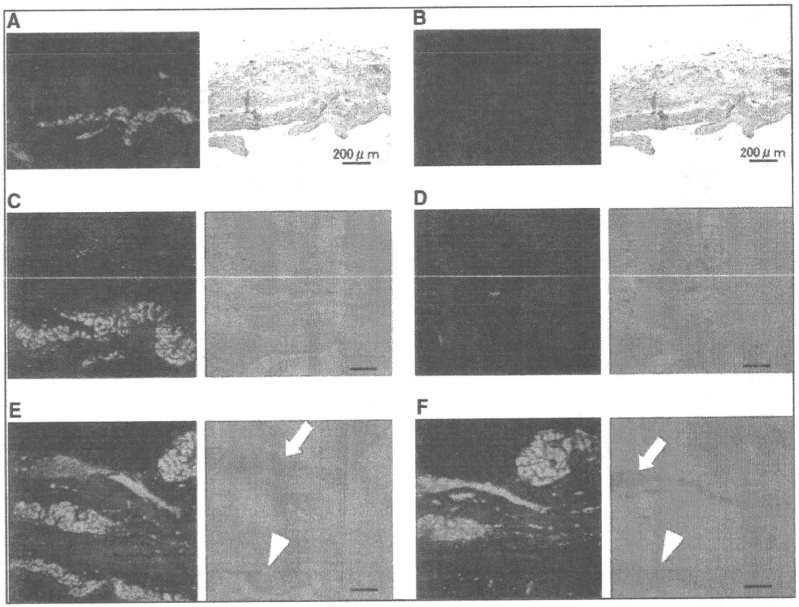

FIG. 4. CLCs differentiate into cardiac muscles *in situ*. Immunofluorescence with anti-α-CA (**A, C, E**) and anti-human-specific cardiac troponin I (**B, D, F**) antibodies, merged with phase contrast. In the hADMSC-derived CLC patch-transplanted groups, two cardiac muscle layers positive for α-CA are observed (**E**, arrow and arrowhead). A large mass of human troponin I-positive myocardium was observed in the CLC-transplanted tissues (**F**, arrows). In the same animals, the internal myocardium layer expressed α-CA but not human troponin I (**E, F**, arrowheads). (**A, B**) Sham-operated MI control group; (**C, D**) noncommitted hADMSC patch-transplanted group; and (**E, F**) CLC patch-transplanted group. Bars = 200 μm.

CLCs can differentiate into cardiomyocytes *in vivo* within the myocardial milieu, resulting in increment of myocardial muscle force. Finally, reconstruction of thick myocardial tissue rescued cardiac dysfunction after MI and improved long-term survival.

The choice of cell source is critical for realizing success in cellular therapy.[18] Liposuction surgeries yield from 100 mL to >3 L of lipoaspirate tissue.[19] The initial isolation of cells from adipose tissue was described by Bjorntorp *et al.*[14] This procedure was since modified to isolate cells from human adipose tissue specimens.[20–22] In this context, Zuk *et al.*[11] reported that the preadipocytes exhibited stem cell features as MSCs, currently known as ADMSCs. Because of the above-stated advantages of procuring cells for therapy from adipose tissues, hADMSCs present a potential and promising source for cellular therapy, even in patients with post-MI severe heart failure.

The *in vitro* differentiation of ADMSCs is now well reported, and experimental findings in recent years suggested considerable therapeutic potential for cellular replacement in the context of acute MI and chronic progressive cardiac disease.[23–27] Stem cells are differentiated into a cardiomyocyte lineage by treatment with 5-azacytidie, retinoic acid, oxytocin, and many other reagents.[28–32] We proposed that DMSO could differentiate hADMSCs into CLCs, based on the differentiation of P19 embryonic stems cells into cardiomyocytes with DMSO.[31–33] It was notable that DMSO is also available in current good manufacturing practice grade. Unfortunately, DMSO-treated hADMSCs did not show spontaneous beating as their terminal differentiation function, but the cells did express the mature markers α-*CA*, *myosin light chain*, and *myosin heavy chain* to a lesser extent. There are no reports of the use of DMSO to commit ADMSCs to a cardiomyocytic lineage. The mechanism by which DMSO elicits its effect on differentiation remains unclear. It is possible that DMSO increases intracellular calcium ion concentration, thereby elevating phosphatidylethanolamine levels in the cells and controlling the distribution of protein kinase C to commit the P19 stem cells.[33–36] These mechanisms should be investigated further in the near future.

The *in vitro* differentiation of ADMSCs has been well reported,[23–27] although only a few reports relate to the differentiation of these cells into cardiomyocytes *in vivo*. Recently,

Miyahara *et al.*[13] reported the use of monolayered ADMSCs for myocardial repair. In their study, rat ADMSCs were isolated and grown as intact monolayer sheets using temperature-responsive culture dishes. Placement of the ADMSC sheets onto a scarred myocardium in rats resulted in diminished scarring and enhanced cardiac structure and function. Histological analysis demonstrated that the engrafted ADMSC sheets grew to form a thickened layer over the infarcted muscle that included newly formed vessels and a few cardiomyocytes. In our study, hADMSC-derived CLCs differentiated into cardiomyocytes in a myocardial milieu, indicated by the immunohistological results in which transplanted cells expressed human troponin I *in vivo*. Newly developed myocardium might augment cardiac function, and thus hADMSC patch transplantation was performed as a control. Cardiac dysfunction was rescued in a short term, although the numbers of cardiomyocytes derived from transplanted cells were low. In this context, Gimble *et al.*[19] suggested that hADMSCs might secrete angiogenic factors and/or antiapoptotic factors.

Transplantation of the hADMSC-derived CLC regenerated the thick myocardial tissues, rescued cardiac dysfunction after MI, and improved long-term survival rate compared with the noncommitted hADMSCs and sham-operated MI controls. The existing literature suggests that ADMSCs can be engrafted and survive within an infarcted myocardial milieu, acquire phenotypic markers consistent with cardiomyocytic and vascular-related lineages, and have a positive impact on structural and functional endpoints.[19,23–27] These are desirable outcomes for cardiac function and survival. However, few reports have applied long-term observation of the transplanted animals. Our study therefore observed the three rat groups for 16 weeks after transplantation. Only CLC transplantation provided the desired outcome at the experimental endpoint. Despite these encouraging results, much progress is needed to realize the hope of cell therapies for myocardial damage. First, delivery of the cell sheets to patients should be optimized for each given disease. Second, the issue of vascularization should be considered in the infracted or affected tissues after transplantation, because many small CLC patches would be necessary for a clinical cure. Finally, the value and impact of CLC patch transplantation should be confirmed in large animal models before embarking on clinical applications.

In conclusion, we showed that the phenotype of hADMSCs could be changed to that of CLCs by induction with DMSO. These hADMSC-derived CLCs engrafted into a scarred myocardium and differentiated into cardiomyocytes. The CLC patch transplantation also resulted in recovery of cardiac function and improved survival rate. Thus, transplantation of hADMSC-derived CLC patches in heart patients might be a potentially effective therapeutic strategy for cardiac tissue regeneration in the near future.

Acknowledgments

This report was supported in part by a grant-in-aid for Yoshiki Sawa from the New Energy and Industrial Technology Development Organization of Japan and in part by a grant-in-aid for Akifumi Matsuyama from the Ministry of Education, Culture, Sports, Science, and Technology of Japan.

Disclosure Statement

No competing financial interests exist.

References

1. Miyagawa, S., Sawa, Y., Taketani, S., Kawaguchi, N., Nakamura, T., Matsuura, N., and Matsuda, H. Myocardial regeneration therapy for heart failure hepatocyte growth factor enhances the effect of cellular cardiomyoplasty. Circulation **105,** 2556, 2002.
2. Miyagawa, S., Matsumiya, G., Funatsu, T., Yoshitatsu, M., Sekiya, N., Fukui, S., Hoashi, T., Hori, M., Yoshikawa, H., Kanakura, Y., Ishikawa, J., Aozasa, K., Kawaguchi, N., Matsuura, N., Myoui, A., Matsuyama, A., Ezoe, S., Iida, H., Matsuda, H., and Sawa, Y. Combined autologous cellular cardiomyoplasty using skeletal myoblasts and bone marrow cells for human ischemic cardiomyopathy with left ventricular assist system implantation: report of a case. Surg Today **39,** 133, 2009.
3. Taylor, D.A. Cell-based myocardial repair: how should we proceed? Int J Cardiol **95,** S8, 2004.
4. Chachques, J.C., Acar, C., Herreros, J., Trainini, J.C., Prosper, F., D'Attellis, N., Fabiani, J.N., and Carpentier, A.F. Cellular cardiomyoplasty: clinical application. Ann Thorac Surg **77,** 1121, 2004.
5. Pallante, B.A., and Edelberg, J.M. Cell sources for cardiac regeneration—which cells and why. Am Heart Hosp J **4,** 95, 2006.
6. Chiu, R.C. MSC immune tolerance in cellular cardiomyoplasty. Semin Thorac Cardiovasc Surg **20,** 115, 2008.
7. Pittenger, M.F., Mackay, A.M., Beck, S.C., Jaiswal, R.K., Douglas, R., Mosca, J.D., Moorman, M.A., Simonetti, D.W., Craig, S., Marshak, D.R. Multilineage potential of adult human mesenchymal stem cells. Science **284,** 143, 1999.
8. Jiang, Y., Jahagirdar, B.N., Reinhardt, R.L., Schwartz, R.E., Keene, C.D., Ortiz-Gonzalez, X.R., Reyes, M., Lenrik, T., Lund, T., Blackstad, M., Du, J., Aldrich, S., Lisberg, A., Low, W.C., Largaespada, D.A., Vertaille, C.M. Pluripotency of mesenchymal stem cells derived from adult marrow. Nature **418,** 41, 2002.
9. Pittenger, M.F., and Martin, B.J. Mesenchymal stem cells and their potential as cardiac therapeutics. Circ Res **95,** 9, 2004.
10. Toma, C., Pittenger, M.F., Cahill, K.S., Byrne, B.J., and Kessler, P.D. Human mesenchymal stem cells differentiate to a cardiomyocyte phenotype in the adult murine heart. Circulation **105,** 93, 2002.
11. Zuk, P.A., Zhu, M., Mizuno, H., Huang, J., Futrell, J.W., Katz, A.J., Benhaim, P., Lorenz, H.P., and Hedrick, M.H. Multilineage cells from human adipose tissue: implications for cell-based therapies. Tissue Eng **7,** 211, 2001.
12. Katz, A.J., Tholpady, A., Tholpady, S.S., Shang, H., and Ogle, R.C. Cell surface and transcriptional characterization of human adipose-derived adherent stromal (hADAS) cells. Stem Cells **23,** 412, 2005.
13. Miyahara, Y., Nagaya, N., Kataoka, M., Yanagawa, B., Tanaka, K., Hao, H., Ishino, K., Ishida, H., Shimizu, T., Kangawa, K., Sano, S., Okano, T., Kitamura, S., and Mori, H. Monolayered mesenchymal stem cells repair scarred myocardium after myocardial infarction. Nat Med **12,** 459, 2006.
14. Bjorntorp, P., Karlsson, M., Pertoft, H., Pettersson, P., Sjostrom, L., and Smith, U. Isolation and characterization of cells from rat adipose tissue developing into adipocytes. J Lipid Res **19,** 316, 1978.

15. Memon, I.A., Sawa, Y., Fukushima, N., Matsumiya, G., Miyagawa, S., Taketani, S., Sakakida, S.K., Kondoh, H., Aleshin, A.N., Shimizu, T., Okano, T., and Matsuda, H. Combined autologous cellular cardiomyoplasty with skeletal myoblasts and bone marrow cells in canine hearts for ischemic cardiomyopathy. J Thorac Cardiovasc Surg **130,** 1333, 2005.
16. Miyagawa, S., Sawa, Y., Sakakida, S., Taketani, S., Kondoh, H., Memon, I.A., Imanishi, Y., Shimizu, T., Okano, T., and Matsuda, H. Tissue cardiomyoplasty using bioengineered contractile cardiomyocyte sheets to repair damaged myocardium: their integration with recipient myocardium. Transplantation **80,** 1586, 2005.
17. Hata, H., Matsumiya, G., Miyagawa, S., Kondoh, H., Kawaguchi, N., Matsuura, N., Shimizu, T., Okano, T., Matsuda, H., and Sawa, Y. Grafted skeletal myoblast sheets attenuate myocardial remodeling in pacing-induced canine heart failure model. J Thorac Cardiovasc Surg **132,** 918, 2006.
18. Murry, C.E., Reinecke, H., and Pabon, L.M. Regeneration gaps: observations on stem cells and cardiac repair. J Am Coll Cardiol **47,** 1777, 2006.
19. Gimble, J.M., Katz, A.J., and Bunnel, B.A. Adipose = derived stem cells for regenerative medicine. Circ Res **100,** 1249, 2007.
20. Deslex, S., Negrel, R., Vannier, C., Etienne, J., and Ailhaud, G. Differentiation of human adipocyte precursors in a chemically defined serum-free medium. Int J Obes **11,** 19, 1987.
21. Hauner, H., Entenmann, G., Wabitsch, M., Gaillard, D., Ailhaud, G., Negrel, R., and Pfeiffer, E.F. Promoting effect of glucocorticoids on the differentiation of human adipocyte precursor cells cultured in a chemically defined medium. J Clin Invest **84,** 1663, 1989.
22. Hauner, H., Wabitsch, M., and Pfeiffer, E.F. Differentiation of adipocyte precursor cells from obese and nonobese adult women and from different adipose tissue sites. Horm Metab Res Suppl **19,** 35, 1988.
23. Parker, A.M., and Katz, A.J. Adipose-derived stem cells for the regeneration of damaged tissues. Expert Opin Biol Ther **6,** 567, 2006.
24. Rangappa, S., Entwistle, J.W., Wechsler, A.S., and Kresh, J.Y. Cardiomyocyte-mediated contact programs human mesenchymal stem cells to express cardiogenic phenotype. J Thorac Cardiovasc Surg **126,** 124, 2003.
25. Gaustad, K.G., Boquest, A.C., Anderson, B.E., Gerdes, A.M., and Collas, P. Differentiation of human adipose tissue stem cells using extracts of rat cardiomyocytes. Biochem Biophys Res Commun **314,** 420, 2004.
26. Planat-Benard, V., Menard, C., Andre, M., Puceat, M., Perez, A., Garcia-Verdugo, J.M., Penicaud, L., and Casteilla, L. Spontaneous cardiomyocyte differentiation from adipose tissue stroma cells. Circ Res **94,** 223, 2004.
27. Strem, B.M., Zhu, M., Alfonso, Z., Daniels, E.J., Schreiber, R., Beygui, R., MacLellan, W.R., Hedrick, M.H., and Fraser, J.K. Expression of cardiomyocytic markers on adipose tissue-derived cells in a murine model of acute myocardial injury. Cytotherapy **7,** 282, 2005.
28. Balana, B., Nicoletti, C., Zahanich, I., Graf, E.M., Christ, T., Boxberger, S., and Ravens, U. 5-Azacytidine induces changes in electrophysiological properties of human mesenchymal stem cells. Cell Res **16,** 949, 2006.
29. Gassanov, N., Er, F., Zagidullin, N., Jankowski, M., Gutkowska, J., and Hoppe, U.C. Retinoid acid-induced effects on atrial and pacemaker cell differentiation and expression of cardiac ion channels. Differentiation **76,** 971, 2008.
30. Paquin, J., Danalache, B.A., Jankowski, M., McCann, S.M., and Gutkowska, J. Oxytocin induces differentiation of P19 embryonic stem cells to cardiomyocytes. Proc Natl Acad Sci USA **99,** 9550, 2002.
31. Fathi, F., Murasawa, S., Hasegawa, S., Asahara, T., Kermani, A.J., and Mowla, S.J. Cardiac differentiation of P19CL6 cells by oxytocin. Int J Cardiol **134,** 75, 2009.
32. Swijnenburg, R.J., van der Bogt, K.E., Sheikh, A.Y., Cao, F., and Wu, J.C. Clinical hurdles for the transplantation of cardiomyocytes derived from human embryonic stem cells: role of molecular imaging. Curr Opin Biotechnol **18,** 38, 2007.
33. Skerjanc, I.S. Cardiac and skeletal muscle development in P19 embryonal carcinoma cells. Trends Cardiovasc Med **9,** 139, 1999.
34. Xu, F.Y., Fandrich, R.R., Nemer, M., Kardami, E., and Hatch, G.M. The subcellular distribution of protein kinase C-alpha, -epsilon, and -zeta isoforms during cardiac cell differentiation. Arch Biochem Biophys **367,** 17, 1999.
35. Xu, F.Y., Kardami, E., Nemer, M., Choy, P.C., and Hatch, G.M. Elevation in phosphatidylethanolamine is an early but not essential event for cardiac cell differentiation. Exp Cell Res **256,** 358, 2000.
36. Monzen, K., Shiojima, I., Hiroi, Y., Kudoh, S., Oka, T., Takimoto, E., Hayashi, D., Hosoda, T., Habara-Ohkubo, A., Nakaoka, T., Fujita, T., Yazaki, Y., and Komuro, I. Bone morphogenetic proteins induce cardiomyocyte differentiation through the mitogen-activated protein kinase kinase kinase TAK1 and cardiac transcription factors Csx/Nkx-2.5 and GATA-4. Mol Cell Biol **19,** 7096, 1999.

Address correspondence to:
Akifumi Matsuyama, M.D., Ph.D.
Department of Somatic Stem Cell Therapy
Foundation for Biomedical Research and Innovation
1-5-4-305 Minatojima-minamimachi
Chuo-ku, Kobe 650-0047
Japan

E-mail: akifumi-matsuyama@umin.ac.jp

Received: June 1, 2009
Accepted: July 21, 2009
Online Publication Date: September 5, 2009

uicc
global cancer control

IJC
International Journal of Cancer

Overexpression of SOCS3 exhibits preclinical antitumor activity against malignant pleural mesothelioma

Kota Iwahori[1,2], Satoshi Serada[1], Minoru Fujimoto[1], Shintaro Nomura[3], Tadashi Osaki[2], Chun Man Lee[4], Hiroyuki Mizuguchi[5], Tsuyoshi Takahashi[1], Barry Ripley[6], Meinoshin Okumura[7], Ichiro Kawase[2], Tadamitsu Kishimoto[6] and Tetsuji Naka[1]

[1] Laboratory for Immune Signal, National Institute of Biomedical Innovation, Osaka, Japan
[2] Department of Respiratory Medicine, Allergy, and Rheumatic Diseases, Osaka University Graduate School of Medicine, Osaka, Japan
[3] Faculty of Animal Bioscience, Nagahama Institute of Bio-Science and Technology, Shiga, Japan
[4] Medical Center for Translational Research, Osaka University Hospital, Osaka, Japan
[5] Laboratory of Gene Transfer and Regulation, National Institute of Biomedical Innovation, Osaka, Japan
[6] Laboratory of Immune Regulation, Osaka University Graduate School of Frontier Biosciences, Osaka, Japan
[7] Department of General Thoracic Surgery, Osaka University Graduate School of Medicine, Osaka, Japan

Malignant pleural mesothelioma (MPM) is an aggressive tumor with poor prognosis for which an effective therapy remains to be established. Our study investigated the therapeutic potential of the suppressor of cytokine signaling 3 (SOCS3), an endogenous inhibitor of intracellular signaling pathways, for treatment of MPM. We infected MPM cells (H226, EHMES-1, MESO-1 and MESO-4) with an adenovirus-expressing SOCS3 (AdSOCS3) to examine the effect of SOCS3 overexpression on MPM cells. SOCS3 overexpression reduced MPM proliferation and induced apoptosis and partial G0/G1 arrest. SOCS3 also inhibited the proliferation of MPM cells *via* multiple signaling pathways including Janus kinase (JAK)/signal transducer and activator of transcription 3 (STAT3), extracellular signal-regulated kinase (ERK), focal adhesion kinase (FAK) and p53 pathways. Notably, AdSOCS3 treatment inhibited tumor growth in an MPM pleural xenograft model. These findings demonstrate that overexpression of SOCS3 has a potent antitumor effect against MPM both *in vitro* and *in vivo* and indicate the potential for clinical use of SOCS3 for MPM treatment.

Malignant pleural mesothelioma (MPM) is an aggressive tumor arising from the mesothelial cells of serosal cavities. MPM may be asymptomatic at the early stage and is sometimes observed incidentally during routine chest radiography. Common symptoms include chest pain and dyspnea, which are caused by tumor invasion of the chest wall or pleural effusion and occur late during disease progression. Although chemotherapy with the drug pemetrexed improves survival time for unresectable MPM patients, the overall median survival time is only 12 months.[1] MPM is often associated with past exposure to asbestos, in which case there is a long latency period, often exceeding 20 years, between first exposure to asbestos and diagnosis of MPM.[2] The number of deaths from MPM is expected to increase in the next 20 years world-wide where heavy use of asbestos has occurred.[2–5] There is thus a growing need for the development of new therapies to treat this disease.

A growing number of studies of MPM tumor biology have established important roles for cytokines involved in tumor growth or the spread of this disease.[6–10] A reported potential molecular target for MPM therapeutics is the interleukin-6 (IL-6)/Janus kinase (JAK)/signal transducer and activator of transcription 3 (STAT3) signaling pathway and

Key words: malignant pleural mesothelioma, suppressor of cytokine signaling 3, gene therapy, signal transducer and activator of transcription 3, p53

Abbreviations: 7-AAD: 7-amino-actinomycin D; DAPI: 4′,6-diamidino-2-phenylindole; DMSO: dimethyl sulfoxide; ERK: extracellular signal-regulated kinase; FAK: focal adhesion kinase; FCS: fetal calf serum; IL-6: interleukin-6; JAK: Janus kinase; MPM: malignant pleural mesothelioma; MOI: multiplicity of infection; MRA: anti-IL-6 receptor antibody; MTS: 3-(4,5-dimethylthiazol-2-yl)-5-(3-carboxymethoxyphenyl)-2-(4-sulfophenyl)-2H-tetrazolium; pfu: plaque-forming units; PI: propidium iodide; SH2: Src homology 2; SHP: SH2-domain-containing tyrosine phosphatase; siRNA: small interfering RNA; SOCS3: suppressor of cytokine signaling 3; STAT3: signal transducer and activator of transcription 3; TUNEL: Terminal deoxynucleotidyl transferase-mediated dUTP nick-end labeling

Grant sponsor: Ministry of Health, Labour and Welfare, Japan, Ministry of Education, Culture, Sports, Science and Technology, Japan
DOI: 10.1002/ijc.25716
History: Received 15 Jun 2010; Accepted 22 Sep 2010; Online 14 Oct 2010

Correspondence to: Tetsuji Naka, Laboratory for Immune Signal, National Institute of Biomedical Innovation, 7-6-8 Saito-Asagi, Ibaraki, Osaka 567-0085, Japan, Tel.: +81-72-641-9843, Fax: +81-72-641-9837, E-mail: tnaka@nibio.go.jp

high-level expression of IL-6 in the pleural fluid of MPM patients.[11,12] The binding of IL-6 to its cognate receptor leads to a conformational change in the receptor that initiates the activation of JAK, which in turn activates the transcription factor STAT3 to dimerize and translocate into the nucleus, thus leading to the initiation of target gene transactivation. This pathway is crucial for the occurrence of hematopoiesis, immune response and oncogenesis.[13] Moreover, dysfunction of the regulatory system for the JAK/STAT3 pathway has been demonstrated to be involved in the development of cancer.[13]

The suppressor of cytokine signaling (SOCS) family proteins[14–16] participate in the negative regulation of multiple signaling pathways including the IL-6/JAK/STAT3 signaling pathway,[17–19] while SOCS3 can bind both the cytokine receptor and JAK, thus facilitating inhibition of the JAK molecule.[20] The restoration of SOCS3 expression in several cancer cell lines was found to effectively suppress tumorigenicity.[21] Because the JAK/STAT3 signaling pathway is frequently activated in a wide variety of human malignancies,[22] SOCS3 gene delivery may represent a novel therapeutic strategy for the treatment of human cancers, including mesothelioma.

In addition to the IL-6/JAK/STAT3 signaling pathway, various other signaling pathways are associated with tumorigenesis in MPM. Among these pathways, activators of oncogenic molecules such as the extracellular signal-regulated kinase (ERK) and focal adhesion kinase (FAK) have been implicated.[23,24] It was reported that SOCS3 participated in the inhibition of ERK phosphorylation and the degradation of FAK.[25–27] SOCS3 can competitively block receptor recruitment of SH2-domain-containing tyrosine phosphatase (SHP-2) to Tyr759 of gp130, thus inhibiting ERK activation. Interactions of SOCS3 with FAK through the Src homology 2 (SH2) domain have been reported to promote polyubiquitination and subsequent degradation of FAK. Because there are multiple abnormalities in signal transduction and genetic differences in individual patients, SOCS3, which, as seen above, is involved in the regulation of multiple signals, is expected to be effective for the treatment of MPM. However, the potential therapeutic benefits of SOCS3 for MPM have not yet been investigated. In the study presented here, we investigated the efficacy of SOCS3 gene delivery for the treatment of MPM.

Material and Methods

Cell lines

Mesothelioma cell lines H28, H226 and H2452 were purchased from American Type Culture Collection (Manassas, VA). Mesothelioma cell line EHMES-1 was kindly provided by Dr. Hironobu Hamada (Ehime University, Ehime, Japan). ACC-MESO-1 (MESO-1) and ACC-MESO-4 (MESO-4) cell lines were purchased from RIKEN BRC cell bank (Tsukuba, Japan). All the cells were cultured in RPMI 1640 (Wako, Osaka, Japan) with 10% fetal calf serum (FCS) (HyClone Laboratories, Logan, UT), 100 IU/mL penicillin and 100 μg/mL streptomycin (Nacalai Tesque, Kyoto, Japan). Human adult mesothelial cells were purchased from Zen-Bio (Research Triangle Park, NC) and cultured in Mesothelial Cell Growth Medium (Zen-Bio). HEK293 cells were obtained from the JCRB Cell Bank (Tokyo, Japan) and cultured in DMEM (Wako) with 10% FCS (HyClone), 100 IU/mL penicillin and 100 μg/mL streptomycin (Nacalai Tesque).

Reagents

Recombinant human IL-6 was kindly provided by Dr. Kazuyuki Yoshizaki (Osaka University, Osaka, Japan), recombinant soluble IL-6 receptor (sIL-6R) and anti-IL-6R monoclonal antibody (tocilizumab, currently known as MRA) were obtained from Chugai Pharmaceutical Co. (Tokyo, Japan). Purified human IgG, purchased from Sigma (St. Louis, MO), was used as control for MRA. JAK inhibitor I and PD98059 were purchased from Calbiochem (La Jolla, CA) and doxorubicin from Wako.

Preparation of adenoviruses

Replication-defective recombinant adenoviral vectors were constructed with the cosmid–adenoviral DNA terminal protein complex method.[28] Adenoviral vectors AdLacZ and adenovirus-expressing SOCS3 (AdSOCS3) were designed to express the LacZ gene and the human SOCS3 gene, respectively, under the control of the CAG promoter (a modified chicken β-actin promoter with a cytomegalovirus immediate early enhancer).[29–31] Solutions of these adenoviral vectors were prepared as described previously and stored at −80°C until use.[32] Adenoviral vectors containing the genes for HA-tagged Y705F dominant-negative STAT3 (AddnSTAT3) were kindly provided by Dr. Akihiko Yoshimura (Keio University, Tokyo, Japan).

X-gal staining

The transduction efficiency of adenoviral vectors was assessed by means of X-gal staining. Cells were cultured in 6-well plates at a density of 1×10^5 cells per well and infected with AdLacZ at the indicated multiplicities of infection (MOIs). X-gal staining was performed 24 hr after infection according to the protocol provided by the manufacturer (Sigma-Aldrich, St. Louis, MO).

Reverse transcription-polymerase chain reaction analysis

Total RNA of cultured cells was isolated with Sepasol-RNA I (Nacalai Tesque) and cDNAs were synthesized from 500 ng of each total RNA preparation with a Quantitect Reverse Transcription kit (QIAGEN, Valencia, CA), all according to the manufacturers' instructions. The TaKaRa Ex Taq (Takara Bio, Otsu, Shiga, Japan) was used for reverse transcription-polymerase chain reaction (RT-PCR) analysis. β-actin was used as a housekeeping gene to evaluate and compare the quality of different cDNA samples. Primers for β-actin (67°C annealing, 33 cycles) were: forward, 5′-AGCCTCGCCTTTGCCGA-3′;

reverse, 5′-CTGGTGCCTGGGGCG-3′. Primers for SOCS3 (55°C annealing, 33 cycles) were: forward, 5′-TCAAGACCTT-CAGCTCCAAG-3′; reverse, 5′-TTGACGCTGAGCGTGAAGAA-3′. And primers for p53 (60°C annealing, 33 cycles) were: forward, 5′-CCCCAGCCAAAGAGAAACC-3′; reverse, 5′-TCCAAGGCCTCATTCAGCTCT-3′. PCR products were detected by means of 1% agarose gel electrophoresis with ethidium bromide staining.

Small interfering RNA transfection

Commercial JAK1 small interfering RNA (siRNA) was obtained from QIAGEN. Cells were transfected with siRNA using Lipofectamine 2000 reagent (Invitrogen, Carlsbad, CA) according to the manufacturer's instructions. Nonspecific siRNA (QIAGEN) was used as a negative control, and the selective silencing of JAK1 was confirmed by Western blot analysis.

Measurement of IL-6 and sIL-6R concentrations in culture supernatant

MPM cells were cultured in 6-well plates at a density of 1×10^5 cells per well and incubated in RPMI 1640 medium containing 0.5% FCS. The concentrations of IL-6 and sIL-6R in the 24-hr culture supernatant were measured by means of Quantikine Colorimetric Sandwich ELISA (R&D Systems, Minneapolis, MN).

SDS-PAGE and western blot analysis

Whole cell protein extract was prepared from MPM cells in RIPA buffer [10 mmol/L Tris-HCl (pH 7.5), 150 mmol/L NaCl, 1% (v/v) NP-40, 0.1% (w/v) SDS, 0.5% (w/v) sodium deoxycholate, 1 mmol/L Na_3VO_4, and 1× protease inhibitor cocktail (Roche Applied Science, Indianapolis, IN)]. Extracted proteins were resolved on SDS-PAGE and transferred to an Immobilon-P Transfer membrane (Millipore, Bedford, MA). The following antibodies were used: antiphospho-STAT3, 1:1,000; anticleaved caspase-3, 1:500; antiphospho-ERK, 1:1,000; anti-ERK, 1:1,000; antiphospho-p53 (Ser46), 1:1,000; antiphospho-p53 (Ser392), 1:1,000 (all from Cell Signaling Technology, Danvers, MA), anti-STAT3, 1:1,000; anti-p53, 1:500; anti-GAPDH, 1:1,000 (all from Santa Cruz Biotechnology, Santa Cruz, CA), antiphospho-FAK (Tyr397) (1:1,000; Biosource, Camarillo, CA), anti-JAK1, 1:1,000; anti-FAK, 1:1,000, anti-p21, 1:1,000 (all from BD Transduction Laboratories, San Jose, CA), antiphosphotyrosine (clone 4G10), 1:1,000 (Upstate Biotechnology, Lake Placid, NY) and anti-SOCS3 antibody (1:500; IBL, Gunma, Japan), followed by a 1:5,000 dilution of donkey antirabbit or 1:5,000 dilution of sheep antimouse horseradish peroxidase-conjugated secondary antibodies (GE Healthcare Bio-Sciences, Piscataway, NJ) and visualized with the Western Lightning ECL reagent (Perkin-Elmer, Boston, MA).

Immunoprecipitation

Cells were lysed in ice-cold RIPA buffer. After clearing of the lysate, anti-p53 antibody (Cell Signaling Technology) was added to the lysate followed by overnight incubation at 4°C. Protein G Sepharose (GE Healthcare Bio-Sciences) was then added and incubated by end-over-end mixing for 2 hr. The beads were washed five times in RIPA buffer and analyzed by Western blotting.

Phospho-kinase array

Expression of phosphorylated proteins was detected with the Proteome Profiler™ Human Phospho-Kinase Array kit (R&D Systems). The procedures were performed according to the manufacturer's protocol using 400 μg protein lysate per array.

MTS assay

MPM cell lines were plated in 96-well plates at a density of 1,000 cells per well and incubated in RPMI 1640 medium containing 10% FCS. After a three-day culture, cell proliferation was evaluated with the 3-(4,5-dimethylthiazol-2-yl)-5-(3-carboxymethoxyphenyl)-2-(4-sulfophenyl)-2H-tetrazolium (MTS) assay (CellTiter 96 aqueous nonradioactive cell proliferation assay; Promega, Madison, WI). MTS color development was measured and analyzed with a microplate reader Model 680 (Bio-Rad Laboratories, Hercules, CA) at a wavelength of 450 nm with a reference wavelength of 750 nm. This assay was performed in triplicate.

Apoptosis assay

MPM cells were grown to confluence to attain synchronization in G1 and subcultured at a lower density (1×10^5 cells in a six-well plate) for 24 hr so that most of the cells were in the S phase. Adenoviral vectors were infected by distributing suspensions of AdSOCS3 or AdLacZ onto cells at a MOI of 40, followed by incubation at 37°C for an additional 72 hr. The cells were then trypsinized and collected with the supernatants, followed by determination of cell viability by means of annexin V and 7-amino-actinomycin D (7-AAD) staining (BD Biosciences, San Jose, CA) using the FACSCanto flow cytometer (BD Biosciences). Data were analyzed with FlowJo software (Tree Star, Ashland, OR). This assay was performed in duplicate.

Cell cycle assay

MPM cells were grown to confluence to attain synchronization in G1 and subcultured at a lower density (1×10^5 cells in a six-well plate) for 24 hr so that most of the cells were in the S phase. Adenoviral vectors were infected by distributing suspensions of AdSOCS3 or AdLacZ onto cells at an MOI of 40, followed by incubation at 37°C for an additional 24 hr. The cells were then trypsinized and collected with the supernatants, after which the cell cycle was determined by means of propidium iodide (PI) staining according to the instructions for the Cycle Test Plus DNA Reagent kits (BD Biosciences) using the FACSCanto flow cytometer. This assay was performed in duplicate.

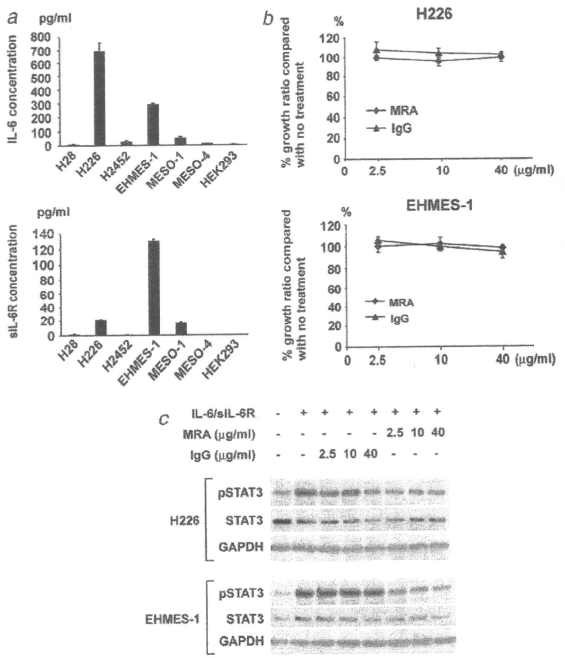

Figure 1. MRA treatment does not inhibit the growth of MPM cells. (*a*) IL-6 and sIL-6R concentrations were measured by using sandwich ELISA. Results are shown as average (columns) + SD (bars). (*b*) Growth curves of H226 and EHMES-1 cells treated with MRA. Cells were cultured in RPMI medium containing 10% FCS with 2.5–40 μg/mL MRA or human IgG. After a 3-day culture, viable cell numbers were counted with the MTS assay. Figures show the average (points) of triplicate wells ± SD (bars). (*c*) Inhibition of phosphor-STAT3 by MRA. H226 and EHMES-1 cells were cultured in RPMI medium containing 0.5% FCS with 2.5–40 μg/mL MRA or human IgG. After a 24-hr culture, the phosphorylation of STAT3 in MPM cells was analyzed after 10-min stimulation with 100 ng/mL of IL-6 and 100 ng/mL of sIL-6R. The lysates from IL-6- and sIL-6R-stimulated cells were analyzed by means of Western blot with antiphospho STAT3 antibody, and subsequently with anti-STAT3 and anti-GAPDH antibody.

Mouse xenograft model

All animal experiments were conducted according to the institutional ethical guidelines for animal experimentation of the National Institute of Biomedical Innovation (Osaka, Japan). Female ICR *nu/nu* mice, 6 to 7 weeks of age, were obtained from Charles River Japan (Yokohama, Japan). The mice were housed for 7 to 14 days and allowed *ad libitum* access to food and water.

For subcutaneous xenograft experiments, we injected 3×10^6 cells in a total volume of 100 μL of 1/1 (v/v) PBS/Matrigel (Becton Dickinson, Bedford, MA) in the flank of ICR *nu/nu* mice. When the tumor sizes reached ~100 mm^3, 1×10^8 plaque-forming units (pfu)/50 μL of AdSOCS3 or AdLacZ was injected intratumorally twice per week. Tumor volumes were determined weekly by measuring in two dimensions, length (L) and width (W), and calculating volume as $(W^2 \times L)/2$.

For pleural xenograft experiments, cells were resuspended in PBS at a density of 1×10^6 cells in a total volume of 150 μL of 1/1 (v/v) PBS/Matrigel (Becton Dickinson). The mice were intrathoracically injected with 150 μL of the cell suspension through a 26-gauge needle. Seven, 14 and 21 days after cell inoculation, 5.0×10^7 plaque-forming units (pfu)/

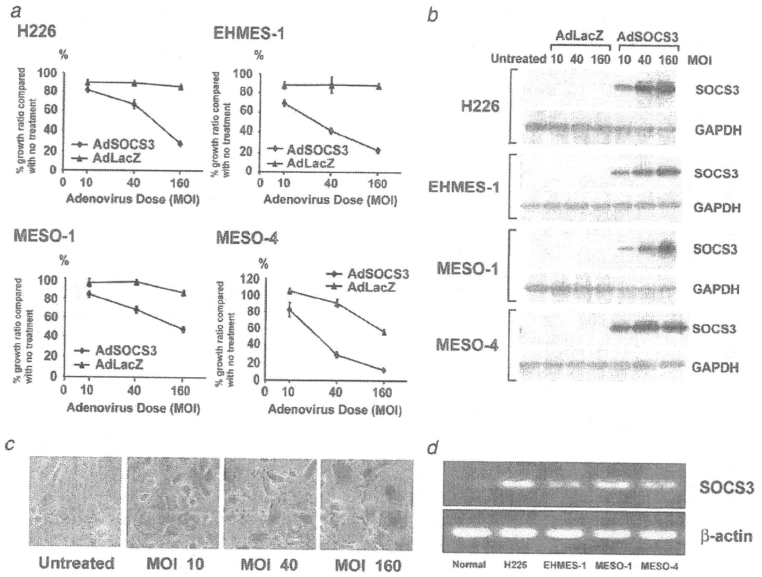

Figure 2. Overexpression of SOCS3 inhibits the growth of MPM cells. (*a*) Growth curves of MPM cells treated with AdSOCS3. Cells were infected with either AdSOCS3 or AdLacZ as control at an MOI of 10–160. Cells were cultured in RPMI 1640 medium containing 10% FCS. After a 3-day culture, viable cell numbers were counted with the MTS assay. Figures show the average (points) of triplicate wells ± SD (bars). (*b*) Expression of SOCS3 as a result of transduction of AdSOCS3. Cells were infected with either AdSOCS3 or AdLacZ as control at an MOI of 10–160. Cells were cultured in RPMI 1640 medium containing 10% FCS. After a 24-hr culture, the cell lysates were analyzed by means of Western blotting using anti-SOCS3 antibody and subsequently with anti-GAPDH antibody. (*c*) Transduction efficiency of the adenoviral vector in H226 cells. H226 cells were infected with AdLacZ at the indicated MOI and stained with X-gal 24 hr after infection. (*d*) Expression of endogenous SOCS3. RT-PCR was used for the assessment of SOCS3 expression.

150 μL of AdSOCS3 or AdLacZ was injected into the thoracic space with the same technique. Twenty-eight days after cell inoculation, the mice were sacrificed and their thoracic spaces examined macroscopically for growths, and tumors detected in the thoracic spaces were removed and weighed.

Immunohistochemistry

Tumors in the thoracic spaces were harvested and paraffin embedded for immunohistochemical analysis using anti-SOCS3 antibody (IBL). Terminal deoxynucleotidyl transferase-mediated dUTP nick-end labeling (TUNEL) assay (with DAPI nuclear counterstaining) for apoptosis was performed using the ApopTag® Fluorescein *in situ* Apoptosis Detection Kit (Chemicon International, Temecula, CA) according to the manufacturer's instructions.

Statistical analysis

Data are shown as mean ± SD for the number of experiments indicated. Student's *t*-test was used for comparison of the data. Differences were considered significant at $p < 0.05$.

Results

MRA treatment has no inhibitory effect on the growth of MPM cells

Reports of high-level expression of IL-6 in the pleural fluid of MPM patients prompted us to investigate the role of this signaling pathway in MPM. To characterize IL-6/sIL-6R levels secreted by MPM cell lines, we used sandwich ELISA for quantitation of IL-6/sIL-6R levels in 24-hr culture supernatants. As shown in Figure 1*a*, H226 and EHMES-1 were identified as cell lines with high IL-6/sIL-6R secretion.

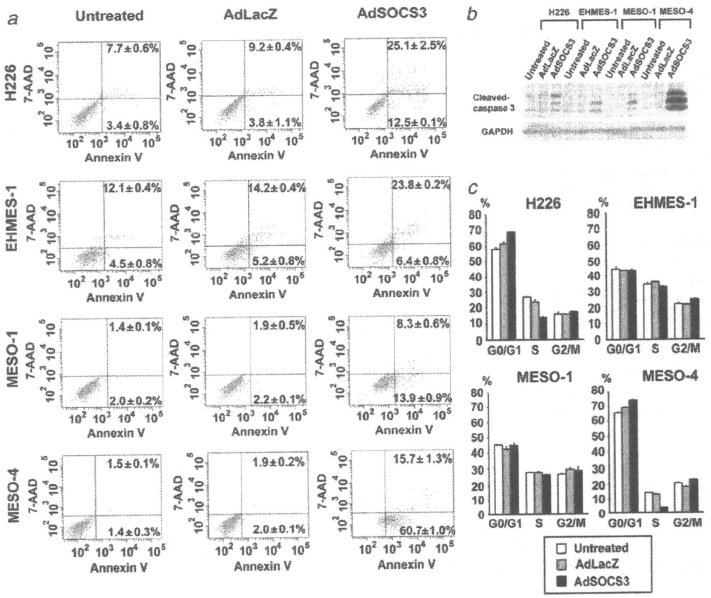

Figure 3. SOCS3 induces apoptosis and G0/G1 arrest in MPM cells. (*a*) Cells were infected with either AdSOCS3 or AdLacZ as control at an MOI of 40. Cells were cultured in RPMI 1640 medium containing 10% FCS for 3 days. Apoptosis was determined by means of annexin V and 7-AAD staining using flow cytometry. Figures show the average of duplicate wells ± SD. (*b*) Cells were infected with either AdSOCS3 or AdLacZ as control at an MOI of 40. Cells were cultured in RPMI 1640 medium containing 10% FCS for 3 days. Whole cell extracts were prepared and immunoblotted with anticleaved caspase-3 antibody. (*c*) Cells were infected with either AdSOCS3 or AdLacZ as control at an MOI of 40. Cells were cultured in RPMI 1640 medium containing 10% FCS for 24 hr. The cell cycle was determined by means of propidium iodide (PI) staining using flow cytometry. Figures show the average (columns) of duplicate wells + SD (bars).

Because it has been reported that IL-6 may represent a therapeutic target for tumorigenesis in MPM cells,[12] we subsequently tested the effect of anti-IL-6R monoclonal antibody (MRA) treatment. For this analysis, we used H226 and EHMES-1 cells which secrete high levels of IL-6. Figure 1*b* shows that MRA did not inhibit cell growth in H226 and EHMES-1 cells. On the other hand, it has been reported that 25 μg/mL of MRA is required for sufficient growth suppression of Lennert's lymphoma-derived T cells which show IL-6–dependent cell growth[12] and we demonstrated that MRA inhibited IL-6-stimulated STAT3 phosphorylation in MPM cells (Fig. 1*c*). These results suggest that, although H226 and EHMES-1 cells secreted high levels of IL-6, IL-6 signaling had little effect on the growth of these cells. However, the role of STAT3 on cell growth in H226 and EHMES-1 cells was not clear since MRA treatment did not inhibit endogenous phosphorylated STAT3 levels in these cells.

Overexpression of SOCS3 inhibits the growth of MPM cells

The JAK/STAT3 pathway is an important signaling pathway negatively regulated by SOCS3. We therefore used a replication-defective recombinant adenoviral vector to investigate the regulation of MPM cell growth by SOCS3. As shown in Figure 2*a*, AdSOCS3 strongly inhibited cell growth in H226, EHMES-1, MESO-1 and MESO-4 cells, while the endogenous SOCS3 expression levels of MPM cells were higher than those of normal mesothelial cells (Fig. 2*d*). This indicates that overexpression of SOCS3 was required for growth inhibition of MPM cells. Because sufficient transduction efficiency of the adenovirus vector and strong expression of

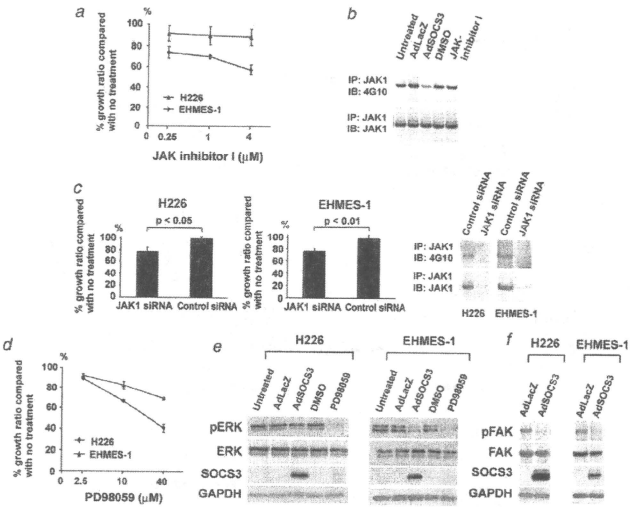

Figure 4. SOCS3 inhibits JAK1, ERK and FAK signaling. (*a*) Growth curves of H226 and EHMES-1 cells treated with JAK inhibitor I. Cells were cultured in RPMI 1640 medium containing 10% FCS with 0.25–4 μM JAK inhibitor I or dimethyl sulfoxide (DMSO) (untreated). After a 3-day culture, viable cell numbers were counted with the MTS assay. Figures show the average (points) of triplicate wells ± SD (bars). (*b*) Inhibition of JAK1 phosphorylation by AdSOCS3. H226 cells were cultured in RPMI 1640 medium containing 0.5% FCS with 1 μM JAK inhibitor I or AdSOCS3 at an MOI of 40. After 24 hr of culturing, 100 ng/mL of IL-6 and 100 ng/mL of sIL-6R were added for 10 min and protein extracts were immunoprecipitated with anti-JAK1 antibody and blotted with antiphosphotyrosine antibody (clone 4G10). (*c*) Growth of H226 and EHMES-1 cells treated with JAK1 siRNA. Cells were treated with either JAK1 siRNA or nonspecific siRNA as control. Cells were cultured in RPMI 1640 medium containing 0.5% FCS, 100 ng/mL of IL-6 and 100 ng/mL of sIL-6R. After a 3-day culture, viable cell numbers were counted with the MTS assay. Figures show the average (columns) of triplicate wells + SD (bars). Protein extracts were immunoprecipitated with anti-JAK1 antibody and blotted with antiphosphotyrosine antibody (clone 4G10) and subsequently with anti-JAK1 antibody. (*d*) Growth curves of H226 and EHMES-1 cells treated with PD98059. Cells were cultured in RPMI 1640 medium containing 10% FCS with 2.5–40 μM PD98059 or dimethyl sulfoxide (DMSO) (untreated). After a 6-day culture, viable cell numbers were counted with the MTS assay. Figures show the average (points) of triplicate wells ± SD (bars). (*e*) Inhibition of ERK phosphorylation by AdSOCS3. H226 and EHMES-1 cells were cultured in RPMI 1640 medium containing 0.5% FCS with 4 μM PD98059 or AdSOCS3 at an MOI of 40. After 24 hr of culturing, protein extracts were blotted with antiphospho-ERK antibody. (*f*) Negative regulation of FAK signaling by SOCS3. H226 and EHMES-1 cells were cultured in RPMI 1640 medium containing 10% FCS with AdSOCS3 at an MOI of 40. After 24 hr of culturing, cells were cultured in RPMI 1640 medium containing 0.5% FCS for an additional 24 hr. Protein extracts were blotted with antiphospho-FAK antibody.

SOCS3 were detected at an MOI of 40 in MPM cells (Figs. 2*b* and 2*c*), we performed subsequent experiments using AdSOCS3 at an MOI of 40.

SOCS3 induces apoptosis and G0/G1 arrest in MPM cells

Next, we investigated the mechanism by which AdSOCS3 inhibited cell growth in H226, EHMES-1, MESO-1 and MESO-4 cells. Since light microscopy findings suggested poor cell viability, apoptosis in these cells was tested by means of annexin V and 7-AAD staining using flow cytometry three days after the addition of AdSOCS3 to the culture. The results of flow cytometric analysis led to the identification of two types of cells: early apoptotic (AnnexinV^+7-AAD^-) and late apoptotic (Annexin V^+7-AAD^+). Compared to treatment with AdLacZ, treatment with AdSOCS3 resulted in elevated

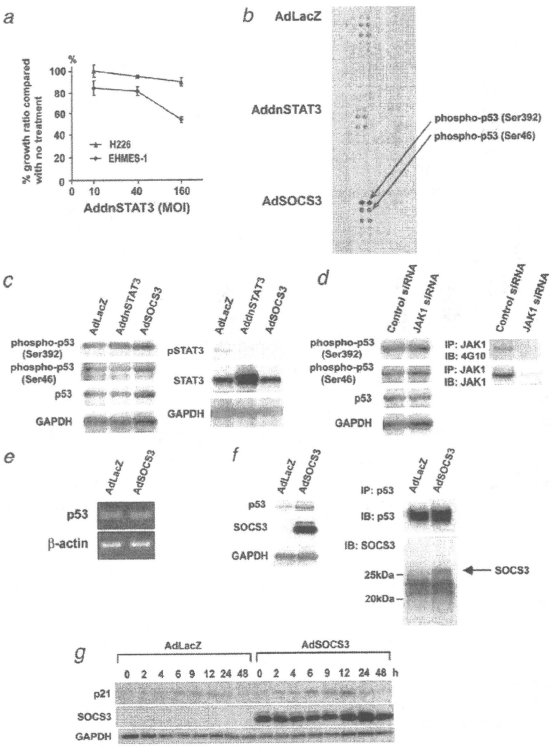

Figure 5. SOCS3 regulates p53 expression in a STAT3-independent manner. (*a*) Growth curves of H226 and EHMES-1 cells treated with AddnSTAT3. Cells were infected with either AddnSTAT3 or AdLacZ as control at an MOI of 10–160. Cells were cultured in RPMI 1640 medium containing 10% FCS. After a 3-day culture, viable cell numbers were counted with the MTS assay. Figures show the average (points) of triplicate wells ± SD (bars). (*b*) Phospho-kinase array revealed that H226 cells treated with AdSOCS3 showed higher levels of phospho-p53 (Ser 392) and phospho-p53 (Ser 46) expression than those treated with AddnSTAT3 or AdLacZ. H226 cells were cultured in RPMI 1640 medium containing 0.5% FCS with AdSOCS3 at an MOI of 40. After 24 hr of culturing, protein extracts were examined with a phospho-kinase array with each phosphorylated protein identified in duplicate. The double-labeled spots in the upper right corner represent the positive controls. (*c*) p53 expression was induced by AdSOCS3. H226 cells were cultured in RPMI 1640 medium containing 0.5% FCS with AdSOCS3 at an MOI of 40. After 24 hr of culturing, protein extracts were probed with antiphospho-p53 (Ser 392), phospho-p53 (Ser 46), p53, phospho-STAT3, STAT3 and GAPDH antibody. (*d*) Influence of JAK1 siRNA on p53 expression. Either JAK1 siRNA or nonspecific siRNA as control was added to H226 cells. Cells were cultured in RPMI 1640 medium containing 0.5% FCS. After 48 hr of culturing, 100 ng/mL of IL-6 and 100 ng/mL of sIL-6R were added for 10 min. The protein extracts were probed with antiphospho-p53 (Ser 392), phospho-p53 (Ser 46), p53 and GAPDH antibody or immunoprecipitated with anti-JAK1 antibody and blotted with antiphosphotyrosine antibody (clone 4G10) and subsequently with anti-JAK1 antibody. (*e*) Expression of p53. RT-PCR was used to determine levels of p53 expression. (*f*) SOCS3 interacts with p53. H226 cells were cultured in RPMI 1640 medium containing 10% FCS with AdSOCS3 at an MOI of 40. After 24 hr of culturing, protein extracts were immunoprecipitated with anti-p53 antibody and immunoblotted with anti-SOCS3 antibody. (*g*) SOCS3 enhances p21 expression. H226 cells were cultured in RPMI 1640 medium containing 10% FCS with AdSOCS3 at an MOI of 40. After 12 hr of culturing, H226 cells were treated with doxorubicin (300 ng/mL) for 0–48 hr. Protein extracts were immunoblotted with anti-p21 antibody.

apoptosis in both early and late apoptotic subsets in H226, EHMES-1, MESO-1 and MESO-4 cells (Fig. 3*a*). Furthermore, cleaved caspase-3, one of the key molecules in apoptosis, was detected in whole cell extracts of H226, EHMES-1, MESO-1 and MESO-4 cells treated with AdSOCS3 (Fig. 3*b*). We therefore conclude that AdSOCS3 induced apoptosis in MPM cells.

In addition to apoptosis, cell cycle regulation is an important mechanism for inhibition of cell growth. To analyze the effect of AdSOCS3 on cell cycle regulation, we infected H226, EHMES-1, MESO-1 and MESO-4 cells with AdSOCS3 and then analyzed cell cycle distribution by means of flow cytometry. When H226 and MESO-4 cells were treated with AdSOCS3, the G0/G1 cell population increased more than in those treated with AdLacZ (Fig. 3*c*).

SOCS3 inhibits JAK1, ERK and FAK signaling

One of the important signaling pathways regulated by SOCS3 is the JAK/STAT3 pathway. We used JAK inhibitor I, which suppresses JAK2 signaling, to investigate the regulation of cell growth by JAK signaling pathways. For this assay, we used H226 and EHMES-1 cell lines (on which MRA had no growth inhibitory effect) to investigate the IL6-independent growth inhibitory effect by SOCS3. As shown in Figure 4*a*, only the growth of EHMES-1 cells, and not of H226 cells, was inhibited by JAK inhibitor I. This suggests that AdSOCS3 inhibited cell growth in H226 cells *via* signaling pathways which were not inhibited by JAK inhibitor I.

To identify the differences between the inhibitory effects of AdSOCS3 and JAK inhibitor I on JAK signaling pathways, we studied changes in the phosphorylation status of JAK1 in H226 cells treated with AdSOCS3 and JAK inhibitor I. Figure 4*b* shows that AdSOCS3 suppressed IL-6–stimulated JAK1 phosphorylation, but that JAK inhibitor I did not affect it. These results lead us to propose that SOCS3 inhibited cell growth in H226 in part by means of negative regulation of JAK1.

We used JAK1 siRNA to evaluate the role of JAK1 signaling pathways in cell growth. As seen in Figure 4*c*, JAK1 siRNA inhibited cell growth in H226 and EHMES-1 cells, suggesting that the growth of H226 cells was partially regulated by JAK1 signaling.

Because it has been reported that SOCS3 inhibits the ERK and FAK signalling pathways, we examined these pathways in H226 and EHMES-1 cells. Figure 4*d* demonstrated that the growth of H226 and EHMES-1 cells was inhibited by the ERK inhibitor PD98059, while ERK phosphorylation was inhibited by AdSOCS3 in these cells (Fig. 4*e*). In addition, AdSOCS3 inhibited phospho-FAK and FAK in H226 and EHMES-1 cells (Fig. 4*f*). We therefore conclude that overexpression of SOCS3 regulates multiple signaling pathways in MPM cells.

SOCS3 regulates p53 expression

We next investigated the role of STAT3 in H226 and EHMES-1 cells and used AddnSTAT3 to examine the regulation of cell growth by STAT3 signaling pathways. As seen in Figure 5*a*, AddnSTAT3 inhibited cell growth in EHMES-1 cells but not in H226 cells. Since this suggests that STAT3 is not involved in the growth of H226 cells, we focused our study on signaling pathways independent of STAT3.

To identify the target molecules of SOCS3 in STAT3-independent pathways, we used a phospho-kinase array to evaluate the expression profile of phosphorylated proteins in H226 cells. Figure 5*b* shows that expression of phospho-p53 (Ser 392) and phospho-p53 (Ser 46) in H226 cells after treatment with AdSOCS3 was higher than in those treated with either AddnSTAT3 or AdLacZ. In addition to phospho-p53, p53 was also highly expressed when treated with AdSOCS3 (Fig. 5*c*). These results suggest that SOCS3 regulated p53 expression.

We next investigated whether JAK1 regulates p53 expression. To this end, we used JAK1 siRNA for the transfection of H226 cells and Western blotting for the examination of p53 expression. As shown in Figure 5*d*, silencing of JAK1 did not influence p53 expression, indicating that JAK1 and p53 are regulated by SOCS3 *via* independent pathways.

Since transfection with AdSOCS3 did not enhance transcription of p53 in H226 cells (Fig. 5*e*), we next investigated whether SOCS3 interacts with p53. After transfection of AdSOCS3 into H226 cells, we detected SOCS3 in the immunoprecipitate of a p53-specific antibody (Fig. 5*f*). In addition, SOCS3 enhanced the expression of p21 which was the target of p53 (Fig. 5*g*). Taken together, these findings suggest that SOCS3 interacts with p53 protein.

SOCS3 exhibits antitumor activity in a mesothelioma xenograft model

We also evaluated the therapeutic effect of AdSOCS3 injection on the growth of subcutaneously or intrathoracically implanted MPM cells in ICR *nu/nu* mice. Of the MPM cell lines used in our study, we were able to establish H226 and MESO-4 xenograft models. Injection of AdSOCS3 vector (1×10^8 pfu/50 μL) intratumorally twice per week reduced tumor volumes compared to tumor volumes in control AdLacZ-injected animals (Fig. 6*a*). Preliminary experiments revealed that when 1×10^6 MPM cells (H226 or MESO-4) were inoculated into the thoracic space, dissemination of tumors was observed in all mice 28 days after cell implantation. Injection of the AdSOCS3 vector (5×10^7 pfu/150 μL) into the thoracic cavity 7, 14 and 21 days after the implantation of 1×10^6 MPM cells (H226 or MESO-4), reduced the weight of tumor nodules compared to the weight of those in control AdLacZ-injected animals (Figs. 6*b* and 6*c*). Finally, Western blot and immunohistochemical analysis indicated that SOCS3 was overexpressed and induced apoptosis in the

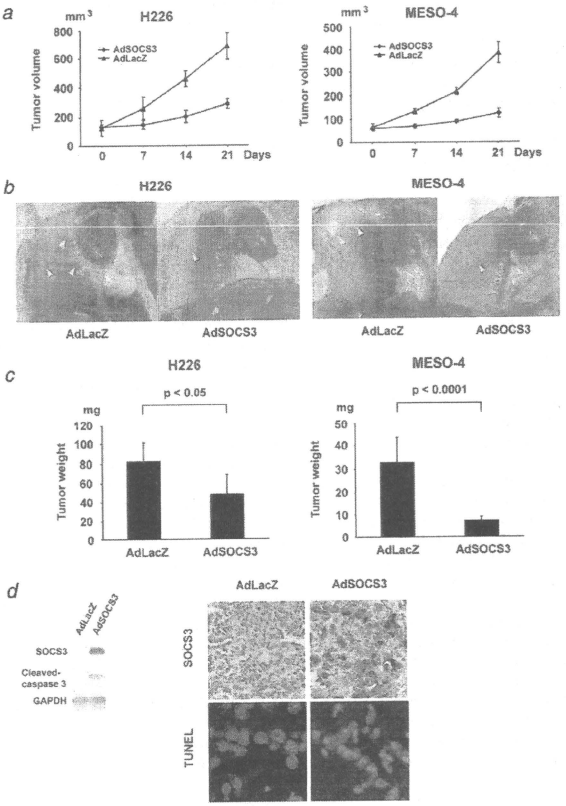

Figure 6. SOCS3 exhibits antitumor activity in a mesothelioma xenograft model. (*a*) Female ICR *nu/nu* mice were intratumorally treated with 1×10^8 pfu of AdSOCS3 or AdLacZ twice per week after the implantation of 3×10^6 H226 or MESO-4 cells subcutaneously in the flank of mice. Tumor volumes were determined weekly. Figures show the average (points) for five animals ± SD (bars). (*b*) Gross appearance of H226 and MESO-4 tumors grown orthotopically in the thoracic spaces. Female ICR *nu/nu* mice were intrathoracically treated with 5×10^7 pfu of AdSOCS3 or AdLacZ for 7, 14 and 21 days after the implantation of 1×10^6 H226 or MESO-4 cells into the pleural space. After 28 days of tumor cell inoculation, the animals were sacrificed and pleural dissemination of the tumor cells was assessed. (*c*) Each tumor nodule found in the thoracic spaces was also weighed. Figures show the average (columns) for eight animals + SD (bars). (*d*) Western blot analysis of SOCS3 and cleaved caspase-3 in H226 tissue from AdSOCS3-injected animals (left panel). The H226 cell bearing animals were treated with AdSOCS3 on day 7 and sacrificed on day 10. The thoracic tumors were analyzed by Western blot. Immunohistochemical analysis of SOCS3 and TUNEL (blue fluorescence = DAPI staining for nuclei; cyan fluorescence = TUNEL positivity) in H226 tissue from AdSOCS3-injected animals (right panel). The animals were treated in the same way as described above.

H226 tissue from AdSOCS3-injected animals (Fig. 6*d*). Immunohistochemical analysis of SOCS3 overexpression and apoptosis in MESO-4 tissue could not be clearly determined, however Western blot analysis showed identical results to that observed in H226 tissue (data not shown). From these results, we conclude that SOCS3 exhibits antitumor activity not only *in vitro* but also *in vivo* in the MPM model. We hope that these findings may lead to the successful clinical application of SOCS3 for MPM treatment.

Discussion

Malignant mesothelioma represents a great challenge to both clinicians and researchers due to its poor prognosis and remarkable resistance to current therapies. Although there have been some improvements in treatment over the past few years, a better understanding of the molecular basis of the disease and of how to improve treatment is required. Among molecular targeted therapies, recently developed tyrosine kinase inhibitors have been tested for MPM but without therapeutic benefit. This is partially explained by the fact that multiple receptor tyrosine kinases are frequently activated in most MM cells.[23] In our study, we showed that SOCS3 inhibited the proliferation of MPM cells through multiple signaling pathways including JAK/STAT3, ERK, FAK and p53 pathways. We observed that SOCS3 did not influence the expression and activation of p38, JNK, Akt or GSK3β proteins in H226 and EHMES-1 cell lines (data not shown). Specifically, we were able to demonstrate that AdSOCS3 inhibits MPM progression in a mouse pleural xenograft model. These data provide new insights into the clinical application of SOCS3 gene delivery for the treatment of MPM.

We also provided evidence that MRA had little effect on proliferation of MPM cells. A recent study by Adachi *et al.*[12] found that MRA is capable of blocking IL-6 signaling and suppresses the cell growth of MPM induced by IL-6/sIL-6R. We hypothesize that MRA was not able to inhibit proliferation of these cells because it did not inhibit signals from other cytokines acting through gp130 or endogenous activated molecules downstream of gp130 involved in proliferation of these cells.

There are several JAK inhibitors, including JAK inhibitor I,[33] but these inhibitors inhibit JAK1 less than they do other JAK family molecules. This may explain why, although JAK1 is involved in H226 cell proliferation, JAK inhibitor I had little effect on proliferation of H226 cells. SOCS3, however, is an effective JAK1 inhibitory molecule and also inhibits proliferation of H226 cells. It has further been reported that JAK2 inhibitors have antitumor effects on various cancer cells.[34] Because of its pan-JAK inhibitory effect,[20] SOCS3 appears to be a promising antitumor molecule.

We were able to show that SOCS3 regulated phospho-p53 (Ser392 and Ser46) and total p53 expression. Functional inactivation of the p53 pathways appears to be a critical requirement for the development of several human cancers.[35] In spite of the fact that mutations in p53 are among the most commonly acquired genetic lesions seen in cancers, p53 mutations are rarely seen in MPM including H226 cells.[36] It has been reported that Ser392 phosphorylation may regulate the oligomerization of p53 and thus its sequence-specific DNA binding,[37,38] while phosphorylation of Ser46 has been implicated in the activation of p53-dependent apoptotic responses.[39,40] The most thoroughly characterized downstream target of p53 activation is the induction of p21 expression, with p21 playing a critical role in the cell cycle checkpoint.[41] In our study, moreover, SOCS3 enhanced p21 expression and induced apoptosis and G0/G1 arrest in MPM cells. In view of these results, we propose that SOCS3 induces apoptosis as well as G0/G1 arrest partially through the p53 pathways in MPM cells.

Recently, it has been reported that SOCS1 activates p53 *via* a direct interaction between the SH2 domain of SOCS1 and the N-terminal transactivation domain of p53,[42] while we were able to show that SOCS3 did not enhance transcription of p53 but interacted with p53. It is thus conceivable that the observed interaction of SOCS3 with p53 may in turn enhance p53 protein stability. Such a mechanism may therefore involve the inhibition of interaction of p53 with other proteins that promote p53 protein degradation.

In our study, we used adenoviral SOCS3 gene transfer to the thoracic cavity in a mouse xenograft pleural tumor model to provide evidence of a potent antitumor effect of SOCS3 *in vivo*. Because MPM locates within the thoracic cavity and rarely displays widespread metastasis, gene transfer to the thoracic cavity makes this tumor uniquely accessible, thus facilitating the direct administration of novel therapeutic agents and subsequent analysis of treatment effects. Clinical trials involving intrapleural administration of adenoviral vectors to MPM patients have demonstrated that intrapleural gene therapy using adenoviral vectors is safe and well tolerated by MPM patients.[43,44]

In conclusion, we demonstrated the antitumor effect of SOCS3 against MPM both *in vitro* and *in vivo*. The results of clinical application of SOCS3 for MPM treatment are eagerly anticipated.

Acknowledgements

This work was supported by a Grant-in-Aid from the Ministry of Health, Labour and Welfare, Japan (T. Naka), a Grant-in-Aid for Young Scientists (B) from the Ministry of Education, Culture, Sports, Science and Technology, Japan (K. Iwahori) and a grant from the Kansai Biomedical Cluster Project in Saito, which is promoted by the Knowledge Cluster Initiative of the Ministry of Education, Culture, Sports, Science and Technology, Japan (T. Naka). We wish to thank Akihito Yokoyama (Kochi University, Kochi, Japan) and Hironobu Hamada (Ehime University, Ehime, Japan) for providing helpful comments on this article, and Namiko Kawakami and Yukako Ito for their secretarial assistance.